RESEARCH ARTICLE

Check for updates

Purely organic phosphor sensitization for efficiency improvement in yellow fluorescent organic light-emitting diodes†

Ho Jin Jang, Cho Long Kim and Jun Yeob Lee [ID] *

Utilization of a purely organic based room-temperature phosphorescent (RTPH) emitter as a sensitizer was studied by employing it in yellow fluorescent organic light-emitting diodes (OLEDs). The RTPH sensitizer can harvest radiative triplet excitons and would transfer them to the yellow fluorescent dopant for efficient fluorescence, just like a conventional phosphorescent sensitizer. The selected RTPH material was 3-(9H-carbazol-9-yl)-10-(p-tolyl)-10H-phenoselenazine (PSez9Cz), which emits at 507 nm by phosphorescence, and the fluorescent dopant was 2,8-di-*tert*-butyl-5,11-bis(4-*tert*-butylphenyl)-6,12-diphenyltetracene (TBRb). The maximum external quantum efficiency of the yellow fluorescent OLEDs was increased from 2.8% to 8.1% by co-doping 10 wt% of RTPH sensitizer and 0.8 wt% of fluorescent dopant due to efficient Förster energy transfer from the RTPH sensitizer to the dopant.

Introduction

Organic light-emitting diodes (OLEDs) are electroluminescent devices with the process of charge recombination and energy relaxation from the excited state to the ground state. Singlet and triplet excitons are generated at a ratio of 1:3 and the emission mechanism can be distinguished by the origin of the excited state for light emission.[1–6] In the case of fluorescent OLEDs, they use only 25% of singlet excitons for emission, wasting 75% of triplet excitons, resulting in low device efficiency.[6] For efficient utilization of both singlet and triplet excitons and corresponding high efficiency in OLEDs, phosphorescent and thermally activated delayed fluorescent (TADF) OLEDs have been developed. In the case of phosphorescent OLEDs (PHOLEDs), heavy metal atoms such as iridium (Ir) or platinum (Pt) in the emitters strongly induce spin orbit coupling (SOC), converting singlet excitons into triplet excitons by intersystem crossing (ISC) and then utilizing all triplet excitons for light emission.[1,6,7] However, those heavy metals are rare and high-cost materials, and phosphor material design is also limited. To overcome this limitation, TADF and room temperature phosphorescent (RTPH) emitters have been investigated as highly efficient emitters utilizing 100% of radiative excitons. In the TADF emitters, triplet excitons are harvested through minimized singlet–triplet energy splitting and reverse intersystem crossing.[2,6,7] In the case of RTPH emitters, organic based RTPH emitters can induce SOC using high atomic number atoms such as halogens, sulfur, and selenium, and then emit light by triplet exciton relaxation.[8–17]

Despite 100% exciton utilization, TADF emitters generally emit from a charge transfer (CT) state through a twisted donor and acceptor structure, inducing a broad emission spectrum and low color purity. To tackle both high color purity and efficient exciton utilization, hyper-fluorescence[18–23] or multi-resonance TADF[24,25] OLEDs have been studied and developed. In particular, in the case of hyper-fluorescence, the TADF material works as a sensitizer and exciton harvester, and transfers 100% of singlet excitons through Förster energy transfer, improving the low efficiency of fluorescent OLEDs. Similarly, there were some OLED sensitization cases with phosphorescent dopant as a sensitizer due to its 100% exciton utilization and allowed triplet to singlet Förster energy transfer.[26–28] However, utilization of the RTPH emitter as a sensitizer was rarely reported although there have been several works about RTPH OLEDs.[14–17]

In this work, we describe RTPH emitter application as a phosphor sensitizer of a fluorescence emitter for improved efficiency in fluorescence OLEDs. A RTPH emitter of 3-(9H-carbazol-9-yl)-10-(p-tolyl)-10H-phenoselenazine (PSez9Cz) was selected as a phosphor sensitizer and 2,8-di-*tert*-butyl-5,11-bis(4-*tert*-butylphenyl)-6,12-diphenyltetracene (TBRb) was a final fluorescent emitter. The yellow fluorescent OLEDs showed enhanced maximum external quantum efficiency (EQE) of 8.1% compared to 2.8% of the conventional fluorescent OLED without the RTPH sensitizer, proving the potential of the RTPH material as a sensitizer.

School of Chemical Engineering, Sungkyunkwan University, 2066 Seobu-ro, Jangan-gu, Suwon, Gyeonggi 16419, Korea. E-mail: leej17@skku.edu

† Electronic supplementary information (ESI) available. See DOI: https://doi.org/10.1039/d2qm00282e
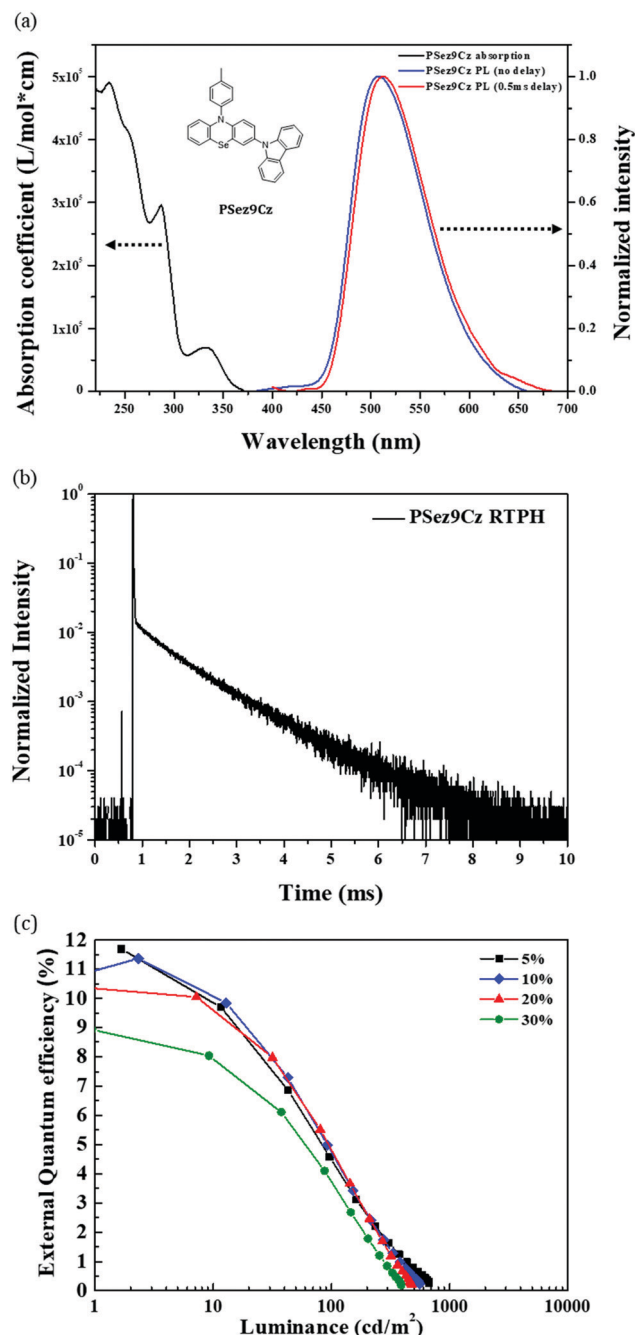
Fig. 1 (a) UV-vis absorption, PL spectrum and molecular structure of PSez9Cz. The absorption spectrum was measured using THF solution. Photoluminescence spectra were measured using 10 wt% PSez9Cz doped mixed host film at room temperature without and with a delay time of 0.5 ms. The mixed host was composed of mCP and TSPO1 (50 : 50). (b) TRPL curves of the 10 wt% PSez9Cz doped mixed host film. Detection wavelength was 513 nm. (c) EQE−luminance curves of PSez9Cz RTPH OLEDs. Device structure was ITO (50 nm)/PEDOT:PSS (60 nm)/TAPC (10 nm)/TCTA (10 nm)/PCzAC (5 nm)/mCP (5 nm)/mixed host : PSez9Cz (25 nm : x wt%)/TSPO1 (5 nm)/TPBi (40 nm)/LiF (1 nm)/Al (200 nm). Doping concentration was 5, 10, 20, and 30 wt%.

Results and discussion

The main purpose of this work is to apply the RTPH emitter as a sensitizer of a fluorescent emitter and to improve the EQE of the fluorescent OLEDs. For efficient Förster energy transfer from the RTPH sensitizer to the fluorophore, spectrum overlap between sensitizer emission and fluorophore absorption is required. The selected sensitizer, PSez9Cz, has phenoselenazine as the main SOC inducing chromophore[14–16] and carbazole as a secondary chromophore. The synthesis and chemical characterization of the PSez9Cz emitter are described in the ESI† (Fig. S1). Basic photophysical data of PSez9CZ are in Fig. 1(a), and Table 1. The ultraviolet-visible (UV-vis) absorption spectrum showed π–π^* absorption peaks at 234 nm and 287 nm, and n–π^* absorption peak at 333 nm. The photoluminescence (PL) spectrum was obtained using a 10 wt% PSez9Cz doped mixed host film. The mixed host was composed of mCP and TSPO1 at a ratio of 50 : 50 to block back energy transfer from the RTPH emitter to the hosts and to balance carriers in the electroluminescence (EL) devices. The phosphorescence spectrum was collected at room temperature after a delay time of 0.5 ms. Both fluorescence and phosphorescence spectra showed almost the same shape and peak wavelength, indicating that PSez9Cz has only one emission process. Also, as shown in Fig. 1(b), a long excited state lifetime of 0.96 ms was measured in the transient photoluminescence (TRPL) by phosphorescence as confirmed by temperature dependent TRPL data in Fig. S2 (ESI†). As the temperature increased from 100 K to 300 K, the decay intensity was gradually decreased by the thermal energy induced quenching process.

Table 1 Photophysical properties of PSez9Cz

	$\lambda_{abs}{}^a$ (nm)	$\lambda_{RTPH}{}^b$ (nm)	$E_T{}^c$ (eV)	HOMO/LUMO^d (eV)	PLQY^e (%)	$\tau_{RTPH}{}^e$ (ms)
PSez9Cz	234, 287, 333	512	2.42	−5.49/−2.06	56.7	0.96

^{a} Absorption spectrum peak of PSez9Cz measured in THF solution. ^{b} 10 wt% PSez9Cz doped mixed host film at room temperature after a delay time of 0.5 ms. The mixed host was composed of mCP and TSPO1 50 : 50. ^{c} Calculated singlet and triplet energy of PSez9Cz from phosphorence peaks. ^{d} HOMO and LUMO energy level measured with cyclic voltammetry (CV). ^{e} Measured using 10 wt% PSeBBz doped mixed host film.

Table 2 Device performance of PSez9Cz RTPH OLEDs

	QE (%)		PE (lm W^{-1})		CE (cd A^{-1})	
	[300 cd m^{-2}]	[Max]	[300 cd m^{-2}]	[Max]	[300 cd m^{-2}]	[Max]
5%	1.7	11.7	2.3	27.3	5.4	39.1
10%	1.5	11.4	2.1	26.7	5.0	37.9
20%	1.4	10.4	2.0	27.2	4.5	34.6
30%	0.8	8.9	1.1	23.3	2.6	29.7

Device structure: ITO (50 nm)/PEDOT:PSS (60 nm)/TAPC (10 nm)/TCTA (10 nm)/PCzAC (5 nm)/mCP (5 nm)/mixed host : PSez9Cz (25 nm : x wt%)/TSPO1 (5 nm)/TPBi (40 nm)/LiF (1 nm)/Al (200 nm). Doping concentration was 5, 10, 20, and 30 wt%.
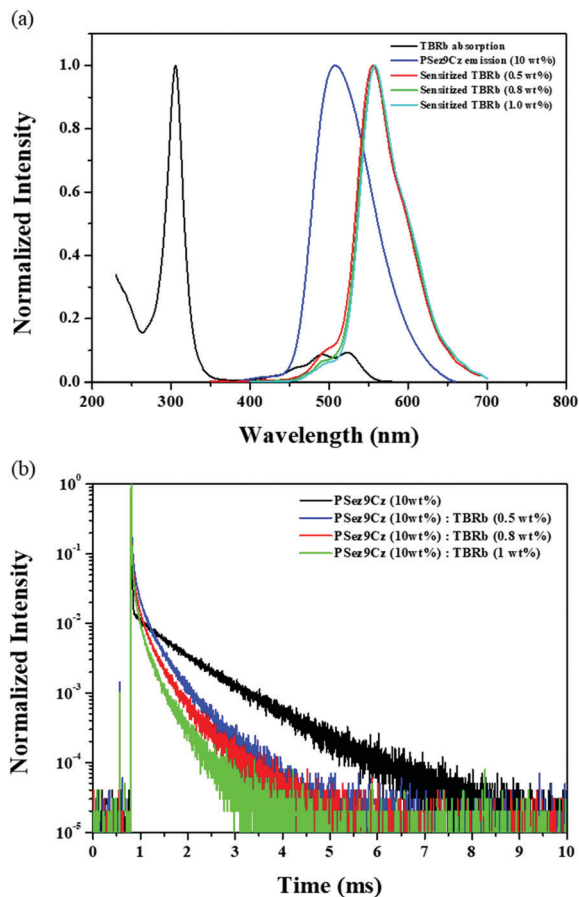
Fig. 2 (a) UV-vis absorption spectra of TBRb and fluorescence spectra of 10 w% PSez9Cz doped in the mixed host with and without TBRb dopant. The doping concentration of the fluorescent dopant was 0.5, 0.8, and 1 wt%. The mixed host was composed of mCP and TSPO1 in 50 : 50. (b) TRPL curves of 10 wt% PSez9Cz doped in the mixed host with and without TBRb dopant. The detection wavelength was 560 nm for the fluorescence emission peak.

The photoluminescence quantum yield (PLQY) of 56.7% was obtained in the 10 wt% PSez9Cz doped mixed host film (Table 1). These results suggest that PSez9Cz is a highly efficient RTPH emitter. Compared to the previous mPhSe RTPH emitter,[15] the PLQY was significantly enhanced by introducing a carbazole group, which behaves as an auxochromophore for efficient emission while maintaining RTPH character of the emission. As shown in Fig. 1(c) and Table 2, high EQE of 11.4% was obtained in the PSez9Cz device. Even though efficiency roll-off is serious in all devices due to its long triplet lifetime inducing triplet–triplet annihilation or triplet-polaron quenching, the high EQE of the PSez9Cz may allow it to be used as the sensitizer of the fluorescent emitter to harvest the singlet excitons by Förster energy transfer. The high EQE exceeding the theoretical limit of the conventional fluorophore (~5%) proves that PSez9Cz effectively harvests triplet excitons for phosphorescence.

To confirm the suitability of PSez9Cz as the sensitizer of yellow-emitting TBRb, overlap between the absorption spectrum of TBRb and emission spectrum of PSez9Cz was investigated. As described in Fig. 2(a), the spectrum overlap between

TBRb absorption and PSez9Cz emission was significant, and the PSez9Cz and TBRb co-doped film showed dominant yellow fluorescence of TBRb, indicating efficient energy transfer from PSez9Cz to TBRb.

The energy transfer was further analyzed by monitoring the TRPL of the PSez9Cz and TBRb co-doped film. In the TRPL curves of Fig. 2(b) and Fig. S3 (ESI†), ns scale fast decay and ms scale slow decay were detected. Comparing the decay of the co-doped film with that of TBRb and PSez9Cz, the fast decay is due to TBRb emission and the slow decay is due to PSez9Cz emission. The energy transfer from the PSez9Cz to TBRb induced the quick decay of the TBRb, while the incomplete energy transfer delivered the slow decay of PSez9Cz. The increase of TBRb doping concentration from 0.5% to 1.0% accelerated the decay of PSez9Cz because of more efficient energy transfer from PSez9Cz to TBRb at high doping concentration. As described in Fig. 3, the triplet exciton energy in the RTPH sensitizer can be transferred not only through Förster energy transfer but also through Dexter energy transfer although Förster energy transfer is preferred for efficient emission.

The phosphor sensitized fluorescent OLEDs were fabricated to confirm the potential of the RTPH emitter as a sensitizer. The device structure and molecular structure of the organic materials are described in Fig. 4. The doping concentration of PSez9Cz was 10 wt% and those of TBRb were 0.5 wt% for Device A and B, 0.8 wt% for Device C and D, and 1 wt% for Device E and F. The devices were divided into a sensitizer free group (Device A, C and E) and a sensitized group (Device B, D and F).

The device performances and EL spectra of the TBRb devices are described in Fig. 5 and Fig. S4 (ESI†) and Table 3. Overall, the device EQE was improved by about 3–4 times in the RTPH sensitized group. As shown in Fig. 5(a), the maximum EQE was
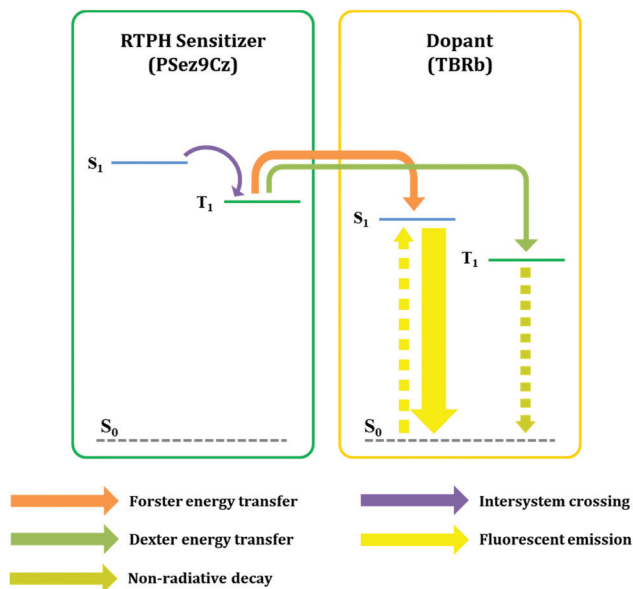

Fig. 3 Scheme of the energy transfer process in the RTPH sensitized fluorescent EML.
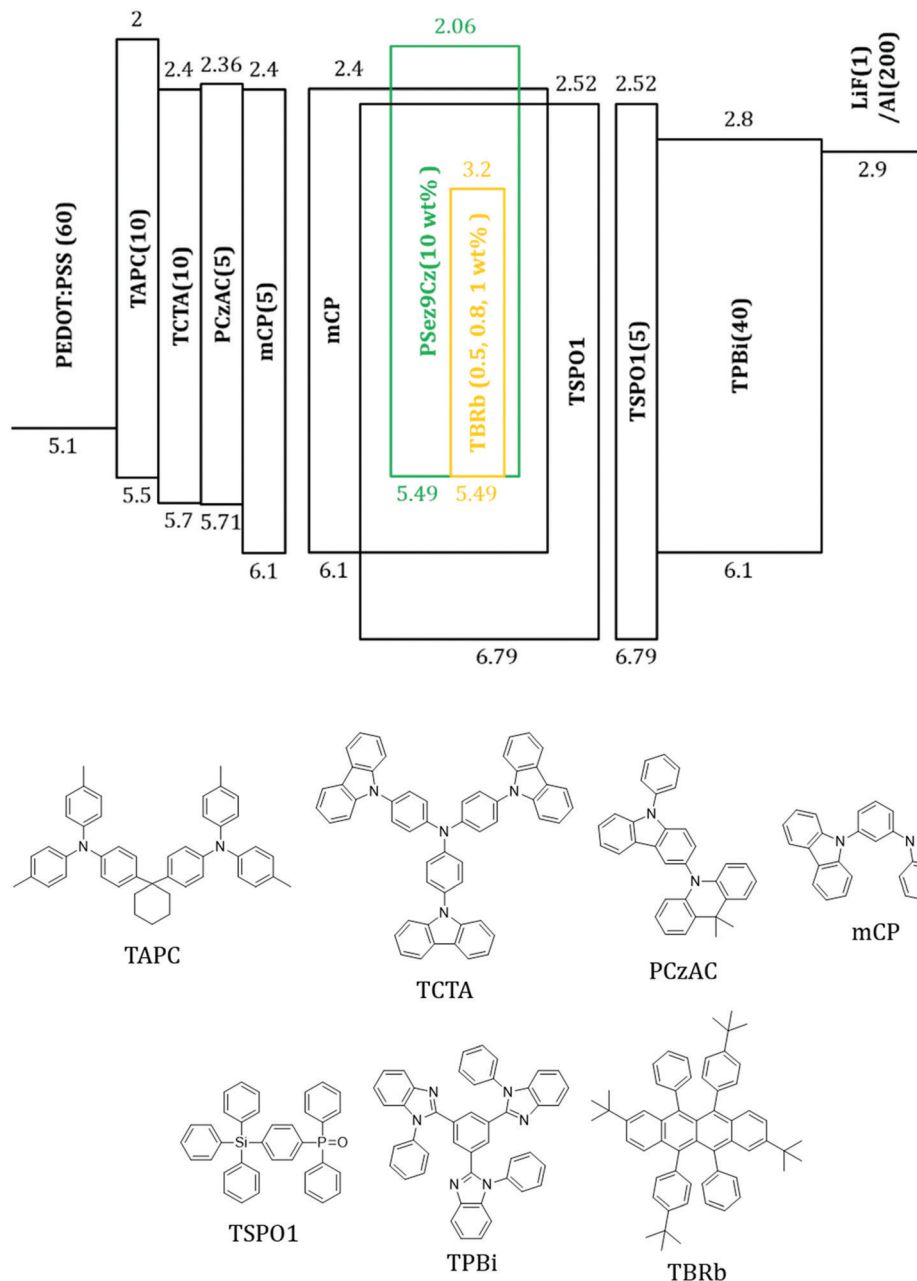
Fig. 4   Device structure of RTPH sensitized yellow fluorescent OLEDs and molecular structures of organic layer materials. The doping concentrations of TBRb were 0.5, 0.8 and 1 wt%, and that of PSez9Cz was 10 wt%.

increased from 2.8% to 8.1% for Device C and D, and from 2.8% to 7.6% for Device E and F.

Although the EQE was enhanced by the sensitization approach, the maximum current density and luminance values were relatively low. There are several reasons for the low luminance of the TBRb devices in this work. First, the mixed host of this work has relatively low hole and electron mobility compared to other hosts reported in the TBRb device. We used the mCP:TSPO1 host to harvest triplet excitons of the pure organic phosphor. The low mobility of mCP and TSPO1 is responsible for the low current density and accompanying low luminance. Second, hole and electron trapping by the

TBRb dopant in the mCP:TSPO1 host limits the current density and luminance. Third, the instability of mCP and TSPO1 host at high current density limits the current density. Fourth, the long triplet exciton lifetime of the PSez9Cz significantly quenches excitons at high luminance, limiting the maximum luminance. The EL spectra described in Fig. 5(b) showed dominant yellow fluorescence with a weak shoulder corresponding to sensitizer emission, inducing blue shift of the color coordinate by 0.02 due to the RTPH emission.

Although the Förster energy transfer from the RTPH sensitizer to TBRb was not complete and the maximum values of device performance were relatively low, the singlet exciton
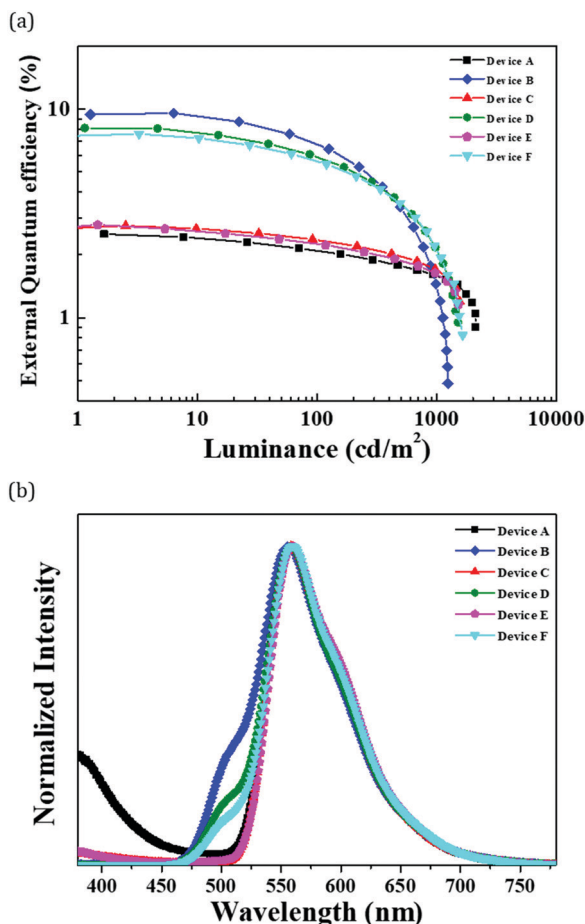
(a)

(b)

Fig. 5 (a) EQE–Luminance curve and (b) EL spectra curves at 500 cd m^{-2} of RTPH sensitized yellow hyperfluorescent OLEDs.

harvesting of TBRb by Förster energy transfer from the PSez9Cz enhanced the EQE of the TBRb devices.

The degree of EQE enhancement by Förster energy transfer was calculated by deconvoluting the EL spectra using the EL spectra of pure PSez9Cz and TBRb. The deconvoluted EL spectra and relative contribution of the PSez9Cz and TBRb are described in Fig. S5 and Table S1 (ESI†). The EQE of the RTPH sensitized device was higher than the simple sum of the PSez9Cz and TBRb EQE, indicating that the EQE enhancement was obviously derived from Förster energy transfer from the RTPH sensitizer to TBRb.

Conclusions

In conclusion, highly efficient PSez9Cz was developed as the RTPH emitter achieving high EQE over 10% through improved PLQY by the secondary auxochromophore. In addition, the potential of PSez9Cz as the sensitizer of TBRb was also confirmed. Efficient energy transfer from the PSez9Cz to TBRb was observed and the EQE of yellow fluorescent OLEDs was enhanced from 2.8% to 8.1%. Therefore, the RTPH emitter can be utilized not only as the emitter but also as the sensitizer for fluorescent OLEDs.

Experimental section

Measurement

Fluorescence and phosphorescence spectra of materials were collected with a fluorescence spectrometer (LS55, PerkinElmer). Absorption spectra of the RTPH sample were measured with a UV-vis spectrometer (V-730 Spectrophotometer, JASCO). TRPL of the RTPH samples was obtained with a fluorescence lifetime spectrometer (C11367 Quantaurus-Tau, Hamamatsu Photonics, Japan) equipped with an ultraviolet-light-emitting diode (280 nm) source system and temperature dependent TRPL was measured by controlling the temperature with a cryostat (Oxford, Optistat DN2).

Device fabrication and analysis

Indium-tin oxide (ITO, 50 nm) coated glass washed in acetone, diluted water, and hot isopropyl alcohol was used as a substrate of the devices. The ITO substrate was modified by ultraviolet ozone treatment before deposition of the hole injection layer. The sensitized devices (B, D, F) were fabricated with the following device structure.: ITO (50 nm)/poly(3,4-ethylenedioxythiophene)–poly(styrenesulfonate) (PEDOT:PSS) (60 nm)/4,4′-cyclohexylidenebis[*N,N*-bis(4-methylphenyl)benzenamine] (TAPC) (10 nm)/tris(4-carbazoyl-9-ylphenyl)amine (TCTA) (10 nm)/9,9-dimethyl-10-(9-phenyl-9*H*-carbazol-3-yl)-9,10-dihydroacridine (PCzAC) (5 nm)/1,3-bis(*N*-carbazolyl)benzene (mCP) (5 nm)/Host:PSez9Cz:TBRb (25 nm : 50 wt% : 10 wt% : *x* wt%)/diphenylphosphine oxide-4-(triphenylsilyl)-phenyl (TSPO1) (5 nm)/1,3,5-tris(1-phenyl-1*H*-benzimidazol-2-yl)benzene (TPBi) (40 nm)/LiF (1 nm)/Al (200 nm). The host was a mixture of mCP and TSPO1 at a ratio of 50:50. The doping concentrations of TBRb were 0.5, 0.7, and 1 wt%. The reference device (A, C, E) structure was ITO (50 nm)/PEDOT:PSS (60 nm)/TAPC (10 nm)/TCTA (10 nm)/PCzAC (5 nm)/mCP (5 nm)/mixed

Table 3 Device performance of RTPH sensitized yellow hyperfluorescent OLEDs

	EQE (%)		PE (lm W^{-1})		CE (cd A^{-1})		
	[500 cd m^{-2}]	[Max]	[500 cd m^{-2}]	[Max]	[500 cd m^{-2}]	[Max]	Color coordinate (x, y)
Device A	1.8	2.5	2.0	4.8	5.1	7.7	(0.43, 0.48)
Device B	3.4	9.6	4.4	22.0	11.1	31.9	(0.42, 0.54)
Device C	2.0	2.8	2.5	5.5	6.5	9.2	(0.46, 0.52)
Device D	3.6	8.1	4.5	18.8	11.7	26.9	(0.44, 0.53)
Device E	1.9	2.8	2.2	5.4	6.1	9.2	(0.47, 0.51)
Device F	3.5	7.6	4.3	17.1	11.6	25.2	(0.45, 0.53)

1986 | *Mater. Chem. Front.*, 2022, **6**, 1982–1988

This journal is © The Royal Society of Chemistry and the Chinese Chemical Society 2022

host : TBRb (25 nm : x wt%)/TSPO1 (5 nm)/TPBi (40 nm)/LiF (1 nm)/ Al (200 nm). All organic materials were thermally deposited at 1 Å s^{-1} under a high vacuum condition ($\sim 10^{-7}$ torr), and LiF and Al were deposited at 0.1 Å s^{-1} and 1 Å s^{-1}, respectively. After the deposition of the cathode, the devices were protected from oxygen and moisture by encapsulation with a cover glass, CaO getter, and epoxy adhesive. Device performances were evaluated with a Keithley electrical source unit and a spectroradiometer (CS-2000, Konica Minolta) for current density, luminance, and EQE measurements.

Conflicts of interest

There are no conflicts to declare.

Acknowledgements

References

1 M. A. Baldo, D. F. O'Brien, Y. You, A. Shoustikov, S. Sibley, M. E. Thompson and S. R. Forrest, Highly efficient phosphorescent emission from organic electroluminescent devices, *Nature*, 1998, **395**, 151–154.

2 P. L. Dos Santos, J. S. Ward, M. R. Bryce and A. P. Monkman, Using Guest–Host Interactions To Optimize the Efficiency of TADF OLEDs, *J. Phys. Chem. Lett.*, 2016, **7**, 3341–3346.

3 B. Geffroy, P. le Roy and C. Prat, Organic light-emitting diode (OLED) technology: materials, devices and display technologies, *Polym. Int.*, 2006, **55**, 572–582.

4 H. J. Jang, J. Y. Lee, J. Kim, J. Kwak and J.-H. Park, Progress of display performances: AR, VR, QLED, and OLED, *J. Inf. Disp.*, 2020, **21**, 1.

5 J. Wang, A. Chepelianskii, F. Gao and N. C. Greenham, Control of exciton spin statistics through spin polarization in organic optoelectronic devices, *Nat. Commun.*, 2012, **3**, 1191.

6 F. B. Dias, K. N. Bourdakos, V. Jankus, K. C. Moss, K. T. Kamtekar, V. Bhalla, J. Santos, M. R. Bryce and A. P. Monkman, Triplet harvesting with 100% efficiency by way of thermally activated delayed fluorescence in charge transfer OLED emitters, *Adv. Mater.*, 2013, **25**, 3707–3714.

7 T. Takahashi, S. Seo, H. Nowatari, S. Hosoumi, T. Ishisone, T. Watabe, S. Mitsumori, N. Ohsawa and S. Yamazaki, Emission mechanism in phosphorescent and fluorescent OLED utilizing energy transfer from exciplex to emitter, *J. Soc. Inf. Disp.*, 2016, **24**, 360–370.

8 S. Guo, W. Dai, X. Chen, Y. Lei, J. Shi, B. Tong, Z. Cai and Y. Dong, Recent Progress in Pure Organic Room Temperature Phosphorescence of Small Molecular Host–Guest Systems, *ACS Mater. Lett.*, 2021, **3**, 379–397.

9 Kenry, C. Chen and B. Liu, Enhancing the performance of pure organic room-temperature phosphorescent luminophores, *Nat. Commun.*, 2019, **10**, 2111.

10 S. Kuila and S. J. George, Phosphorescence Energy Transfer: Ambient Afterglow Fluorescence from Water-Processable and Purely Organic Dyes via Delayed Sensitization, *Angew. Chem., Int. Ed.*, 2020, **59**, 9393–9397.

11 J. Wang, J. Liang, Y. Xu, B. Liang, J. Wei, C. Li, X. Mu, K. Ye and Y. Wang, Purely Organic Phosphorescence Emitter-Based Efficient Electroluminescence Devices, *J. Phys. Chem. Lett.*, 2019, **10**, 5983–5988.

12 X. Yan, H. Peng, Y. Xiang, J. Wang, L. Yu, Y. Tao, H. Li, W. Huang and R. Chen, Recent Advances on Host–Guest Material Systems toward Organic Room Temperature Phosphorescence, *Small*, 2022, **18**, 2104073.

13 Z. A. Yan, X. Lin, S. Sun, X. Ma and H. Tian, Activating Room-Temperature Phosphorescence of Organic Luminophores via External Heavy-Atom Effect and Rigidity of Ionic Polymer Matrix, *Angew. Chem., Int. Ed.*, 2021, **60**, 19735–19739.

14 H. J. Jang, C. R. Kim and J. Y. Lee, Emission color management of dual emitting organic light-emitting diodes by selective switching of phosphorescence through host engineering, *J. Ind. Eng. Chem.*, 2021, **98**, 270–274.

15 C. L. Kim, J. Jeong, H. J. Jang, K. H. Lee, S.-T. Kim, M.-H. Baik and J. Y. Lee, Purely organic phosphorescent organic light emitting diodes using alkyl modified phenoselenazine, *J. Mater. Chem. C*, 2021, **9**, 8233–8238.

16 C. L. Kim, J. Jeong, D. R. Lee, H. J. Jang, S. T. Kim, M. H. Baik and J. Y. Lee, Dual Mode Radiative Transition from a Phenoselenazine Derivative and Electrical Switching of the Emission Mechanism, *J. Phys. Chem. Lett.*, 2020, **11**, 5591–5600.

17 D. R. Lee, S. H. Han and J. Y. Lee, Metal-free and purely organic phosphorescent light-emitting diodes using phosphorescence harvesting hosts and organic phosphorescent emitters, *J. Mater. Chem. C*, 2019, **7**, 11500–11506.

18 H. Abroshan, V. Coropceanu and J.-L. Brédas, Hyperfluorescence-Based Emission in Purely Organic Materials: Suppression of Energy-Loss Mechanisms via Alignment of Triplet Excited States, *ACS Mater. Lett.*, 2020, **2**, 1412–1418.

19 Y. H. Jung, D. Karthik, H. Lee, J. H. Maeng, K. J. Yang, S. Hwang and J. H. Kwon, A New BODIPY Material for Pure Color and Long Lifetime Red Hyperfluorescence Organic Light-Emitting Diode, *ACS Appl. Mater. Interfaces*, 2021, **13**, 17882–17891.

20 W. J. Chung and J. Y. Lee, The role of the bulky blocking unit of the fluorescent emitter in efficient green hyperfluorescent organic light-emitting diodes, *J. Inf. Disp.*, 2021, **22**, 49–54.

21 W. Song and K. S. Yook, Hyperfluorescence-based full fluorescent white organic light-emitting diodes, *J. Ind. Eng. Chem.*, 2018, **61**, 445–448.

22 D. Berenis, G. Kreiza, S. Juršėnas, E. Kamarauskas, V. Ruibys, O. Bobrovas, P. Adomėnas and K. Kazlauskas, Different RISC rates in benzoylpyridine-based TADF compounds and their implications for solution-processed OLEDs, *Dyes Pigm.*, 2020, **182**, 108579.

23 C.-Y. Chan, M. Tanaka, Y.-T. Lee, Y.-W. Wong, H. Nakanotani, T. Hatakeyama and C. Adachi, Stable pure-blue hyperfluorescence organic light-emitting diodes

with high-efficiency and narrow emission, *Nat. Photonics*, 2021, **15**, 203–207.

24 D. Sun, S. M. Suresh, D. Hall, M. Zhang, C. Si, D. B. Cordes, A. M. Z. Slawin, Y. Olivier, X. Zhang and E. Zysman-Colman, The design of an extended multiple resonance TADF emitter based on a polycyclic amine/carbonyl system, *Mater. Chem. Front.*, 2020, **4**, 2018–2022.

25 Y. Zhang, D. Zhang, J. Wei, Z. Liu, Y. Lu and L. Duan, Multi-Resonance Induced Thermally Activated Delayed Fluorophores for Narrowband Green OLEDs, *Angew. Chem., Int. Ed.*, 2019, **58**, 16912–16917.

26 H. G. Kim, H. Shin, Y. H. Ha, R. Kim, S. K. Kwon, Y. H. Kim and J. J. Kim, Triplet Harvesting by a Fluorescent Emitter Using a Phosphorescent Sensitizer for Blue Organic-Light-Emitting Diodes, *ACS Appl. Mater. Interfaces*, 2019, **11**, 26–30.

27 K. H. Lee and J. Y. Lee, Phosphor sensitized thermally activated delayed fluorescence organic light-emitting diodes with ideal deep blue device performances, *J. Mater. Chem. C*, 2019, **7**, 8562–8568.

28 S. Nam, J. W. Kim, H. J. Bae, Y. M. Maruyama, D. Jeong, J. Kim, J. S. Kim, W. J. Son, H. Jeong, J. Lee, S. G. Ihn and H. Choi, Improved Efficiency and Lifetime of Deep-Blue Hyperfluorescent Organic Light-Emitting Diode using Pt(ɪɪ) Complex as Phosphorescent Sensitizer, *Adv. Sci.*, 2021, **8**, 2100586.

This journal is © The Royal Society of Chemistry and the Chinese Chemical Society 2022